Rapid Communications

Measurement of $e^+e^- \to K\bar{K}J/\psi$ cross sections at center-of-mass energies from 4.189 to 4.600 GeV

M. Ablikim,[1] M. N. Achasov,[9,d] S. Ahmed,[14] M. Albrecht,[4] A. Amoroso,[50a,50c] F. F. An,[1] Q. An,[47,39] J. Z. Bai,[1] O. Bakina,[24] R. Baldini Ferroli,[20a] Y. Ban,[32] D. W. Bennett,[19] J. V. Bennett,[5] N. Berger,[23] M. Bertani,[20a] D. Bettoni,[21a] J. M. Bian,[45] F. Bianchi,[50a,50c] E. Boger,[24,b] I. Boyko,[24] R. A. Briere,[5] H. Cai,[52] X. Cai,[1,39] O. Cakir,[42a] A. Calcaterra,[20a] G. F. Cao,[1,43] S. A. Cetin,[42b] J. Chai,[50c] J. F. Chang,[1,39] G. Chelkov,[24,b,c] G. Chen,[1] H. S. Chen,[1,43] J. C. Chen,[1] M. L. Chen,[1,39] P. L. Chen,[48] S. J. Chen,[30] X. R. Chen,[27] Y. B. Chen,[1,39] X. K. Chu,[32] G. Cibinetto,[21a] H. L. Dai,[1,39] J. P. Dai,[35,h] A. Dbeyssi,[14] D. Dedovich,[24] Z. Y. Deng,[1] A. Denig,[23] I. Denysenko,[24] M. Destefanis,[50a,50c] F. De Mori,[50a,50c] Y. Ding,[28] C. Dong,[31] J. Dong,[1,39] L. Y. Dong,[1,43] M. Y. Dong,[1,39,43] Z. L. Dou,[30] S. X. Du,[54] P. F. Duan,[1] J. Fang,[1,39] S. S. Fang,[1,43] X. Fang,[47,39] Y. Fang,[1] R. Farinelli,[21a,21b] L. Fava,[50b,50c] S. Fegan,[23] F. Feldbauer,[23] G. Felici,[20a] C. Q. Feng,[47,39] E. Fioravanti,[21a] M. Fritsch,[23,14] C. D. Fu,[1] Q. Gao,[1] X. L. Gao,[47,39] Y. Gao,[41] Y. G. Gao,[6] Z. Gao,[47,39] I. Garzia,[21a] K. Goetzen,[10] L. Gong,[31] W. X. Gong,[1,39] W. Gradl,[23] M. Greco,[50a,50c] M. H. Gu,[1,39] S. Gu,[15] Y. T. Gu,[12] A. Q. Guo,[1] L. B. Guo,[29] R. P. Guo,[1,43] Y. P. Guo,[23] Z. Haddadi,[26] S. Han,[52] X. Q. Hao,[15] F. A. Harris,[44] K. L. He,[1,43] X. Q. He,[46] F. H. Heinsius,[4] T. Held,[4] Y. K. Heng,[1,39,43] T. Holtmann,[4] Z. L. Hou,[1] C. Hu,[29] H. M. Hu,[1,43] T. Hu,[1,39,43] Y. Hu,[1] G. S. Huang,[47,39] J. S. Huang,[15] X. T. Huang,[34] X. Z. Huang,[30] Z. L. Huang,[28] T. Hussain,[49] W. Ikegami Andersson,[51] Q. Ji,[1] Q. P. Ji,[15] X. B. Ji,[1,43] X. L. Ji,[1,39] X. S. Jiang,[1,39,43] X. Y. Jiang,[31] J. B. Jiao,[34] Z. Jiao,[17] D. P. Jin,[1,39,43] S. Jin,[1,43] T. Johansson,[51] A. Julin,[45] N. Kalantar-Nayestanaki,[26] X. L. Kang,[1] X. S. Kang,[31] M. Kavatsyuk,[26] B. C. Ke,[5] T. Khan,[47,39] P. Kiese,[23] R. Kliemt,[10] L. Koch,[25] O. B. Kolcu,[42b,f] B. Kopf,[4] M. Kornicer,[44] M. Kuemmel,[4] M. Kuhlmann,[4] A. Kupsc,[51] W. Kühn,[25] J. S. Lange,[25] M. Lara,[19] P. Larin,[14] L. Lavezzi,[50c] S. Leiber,[4] H. Leithoff,[23] C. Leng,[50c] C. Li,[51] Cheng Li,[47,39] D. M. Li,[54] F. Li,[1,39] F. Y. Li,[32] G. Li,[1] H. B. Li,[1,43] H. J. Li,[1,43] J. C. Li,[1] J. Q. Li,[4] Jin Li,[33] Kang Li,[13] Ke Li,[34] Lei Li,[3] P. L. Li,[47,39] P. R. Li,[43,7] Q. Y. Li,[34] T. Li,[34] W. D. Li,[1,43] W. G. Li,[1] X. L. Li,[34] X. N. Li,[1,39] X. Q. Li,[31] Z. B. Li,[40] H. Liang,[47,39] Y. F. Liang,[37] Y. T. Liang,[25] G. R. Liao,[11] D. X. Lin,[14] B. Liu,[35,h] B. J. Liu,[1] C. X. Liu,[1] D. Liu,[47,39] F. H. Liu,[36] Fang Liu,[1] Feng Liu,[6] H. B. Liu,[12] H. M. Liu,[1,43] Huanhuan Liu,[1] Huihui Liu,[16] J. B. Liu,[47,39] J. P. Liu,[52] J. Y. Liu,[1,43] K. Liu,[41] K. Y. Liu,[28] Ke Liu,[6] L. D. Liu,[32] P. L. Liu,[1,39] Q. Liu,[43] S. B. Liu,[47,39] X. Liu,[27] Y. B. Liu,[31] Z. A. Liu,[1,39,43] Zhiqing Liu,[23] Y. F. Long,[32] X. C. Lou,[1,39,43] H. J. Lu,[17] J. G. Lu,[1,39] Y. Lu,[1] Y. P. Lu,[1,39] C. L. Luo,[29] M. X. Luo,[53] T. Luo,[44] X. L. Luo,[1,39] X. R. Lyu,[43] F. C. Ma,[28] H. L. Ma,[1] L. L. Ma,[34] M. M. Ma,[1,43] Q. M. Ma,[1] T. Ma,[1] X. N. Ma,[31] X. Y. Ma,[1,39] Y. M. Ma,[34] F. E. Maas,[14] M. Maggiora,[50a,50c] Q. A. Malik,[49] Y. J. Mao,[32] Z. P. Mao,[1] S. Marcello,[50a,50c] J. G. Messchendorp,[26] G. Mezzadri,[21b] J. Min,[1,39] T. J. Min,[1] R. E. Mitchell,[19] X. H. Mo,[1,39,43] Y. J. Mo,[6] C. Morales Morales,[14] G. Morello,[20a] N. Yu. Muchnoi,[9,d] H. Muramatsu,[45] P. Musiol,[4] A. Mustafa,[4] Y. Nefedov,[24] F. Nerling,[10] I. B. Nikolaev,[9,d] Z. Ning,[1,39] S. Nisar,[8] S. L. Niu,[1,39] X. Y. Niu,[1,43] S. L. Olsen,[33,j] Q. Ouyang,[1,39,43] S. Pacetti,[20b] Y. Pan,[47,39] M. Papenbrock,[51] P. Patteri,[20a] M. Pelizaeus,[4] J. Pellegrino,[50a,50c] H. P. Peng,[47,39] K. Peters,[10,g] J. Pettersson,[51] J. L. Ping,[29] R. G. Ping,[1,43] R. Poling,[45] V. Prasad,[47,39] H. R. Qi,[2] M. Qi,[30] S. Qian,[1,39] C. F. Qiao,[43] J. J. Qin,[43] N. Qin,[52] X. S. Qin,[4] Z. H. Qin,[1,39] J. F. Qiu,[1] K. H. Rashid,[49,i] C. F. Redmer,[23] M. Richter,[4] M. Ripka,[23] G. Rong,[1,43] Ch. Rosner,[14] X. D. Ruan,[12] A. Sarantsev,[24,e] M. Savrié,[21b] C. Schnier,[4] K. Schoenning,[51] W. Shan,[32] M. Shao,[47,39] C. P. Shen,[2] P. X. Shen,[31] X. Y. Shen,[1,43] H. Y. Sheng,[1] M. R. Shepherd,[19] J. J. Song,[34] W. M. Song,[34] X. Y. Song,[1] S. Sosio,[50a,50c] C. Sowa,[4] S. Spataro,[50a,50c] G. X. Sun,[1] J. F. Sun,[15] S. S. Sun,[1,43] X. H. Sun,[1] Y. J. Sun,[47,39] Y. K. Sun,[47,39] Y. Z. Sun,[1] Z. J. Sun,[1,39] Z. T. Sun,[19] C. J. Tang,[37] G. Y. Tang,[1] X. Tang,[1] I. Tapan,[42c] M. Tiemens,[26] B. Tsednee,[22] I. Uman,[42d] G. S. Varner,[44] B. Wang,[1] B. L. Wang,[43] D. Wang,[32] D. Y. Wang,[32] Dan Wang,[43] K. Wang,[1,39] L. L. Wang,[1] L. S. Wang,[1] M. Wang,[34] Meng Wang,[1,43] P. Wang,[1] P. L. Wang,[1] W. P. Wang,[47,39] X. F. Wang,[41] Y. Wang,[38] Y. D. Wang,[14] Y. F. Wang,[1,39,43] Y. Q. Wang,[23] Z. Wang,[1,39] Z. G. Wang,[1,39] Z. H. Wang,[47,39] Z. Y. Wang,[1] Zongyuan Wang,[1,43] T. Weber,[23] D. H. Wei,[11] P. Weidenkaff,[23] S. P. Wen,[1] U. Wiedner,[4] M. Wolke,[51] L. H. Wu,[1] L. J. Wu,[1,43] Z. Wu,[1,39] L. Xia,[47,39] X. Xia,[34] Y. Xia,[18] D. Xiao,[1] H. Xiao,[48] Y. J. Xiao,[1,43] Z. J. Xiao,[29] Y. G. Xie,[1,39] Y. H. Xie,[6] X. A. Xiong,[1,43] Q. L. Xiu,[1,39] G. F. Xu,[1] J. J. Xu,[1,43] L. Xu,[1] Q. J. Xu,[13] Q. N. Xu,[43] X. P. Xu,[38] L. Yan,[50a,50c] W. B. Yan,[47,39] W. C. Yan,[47,39] Y. H. Yan,[18] H. J. Yang,[35,h] H. X. Yang,[1] L. Yang,[52] Y. H. Yang,[30] Y. X. Yang,[11] Yifan Yang,[1,43] M. Ye,[1,39] M. H. Ye,[7] J. H. Yin,[1] Z. Y. You,[40] B. X. Yu,[1,39,43] C. X. Yu,[31] J. S. Yu,[27] C. Z. Yuan,[1,43] Y. Yuan,[1] A. Yuncu,[42b,a] A. A. Zafar,[49] A. Zallo,[20a] Y. Zeng,[18] Z. Zeng,[47,39] B. X. Zhang,[1] B. Y. Zhang,[1,39] C. C. Zhang,[1] D. H. Zhang,[1] H. H. Zhang,[40] H. Y. Zhang,[1,39] J. Zhang,[1,43] J. L. Zhang,[1] J. Q. Zhang,[1] J. W. Zhang,[1,39,43] J. Y. Zhang,[1] J. Z. Zhang,[1,43] K. Zhang,[1,43] L. Zhang,[41] S. Q. Zhang,[31] X. Y. Zhang,[34] Y. H. Zhang,[1,39] Y. T. Zhang,[47,39] Yang Zhang,[1] Yao Zhang,[1] Yu Zhang,[43] Z. H. Zhang,[6] Z. P. Zhang,[47] Z. Y. Zhang,[52] G. Zhao,[1] J. W. Zhao,[1,39] J. Y. Zhao,[1,43] J. Z. Zhao,[1,39] Lei Zhao,[47,39] Ling Zhao,[1] M. G. Zhao,[31] Q. Zhao,[1] S. J. Zhao,[54] T. C. Zhao,[1] Y. B. Zhao,[1,39] Z. G. Zhao,[47,39] A. Zhemchugov,[24,b]

B. Zheng,[48] J. P. Zheng,[1,39] W. J. Zheng,[34] Y. H. Zheng,[43] B. Zhong,[29] L. Zhou,[1,39] X. Zhou,[52] X. K. Zhou,[47,39] X. R. Zhou,[47,39] X. Y. Zhou,[1] Y. X. Zhou,[12] J. Zhu,[31] K. Zhu,[1] K. J. Zhu,[1,39,43] S. Zhu,[1] S. H. Zhu,[46] X. L. Zhu,[41] Y. C. Zhu,[47,39] Y. S. Zhu,[1,43] Z. A. Zhu,[1,43] J. Zhuang,[1,39] L. Zotti,[50a,50c] B. S. Zou,[1] and J. H. Zou[11]

(BESIII Collaboration)

[1]*Institute of High Energy Physics, Beijing 100049, People's Republic of China*
[2]*Beihang University, Beijing 100191, People's Republic of China*
[3]*Beijing Institute of Petrochemical Technology, Beijing 102617, People's Republic of China*
[4]*Bochum Ruhr-University, D-44780 Bochum, Germany*
[5]*Carnegie Mellon University, Pittsburgh, Pennsylvania 15213, USA*
[6]*Central China Normal University, Wuhan 430079, People's Republic of China*
[7]*China Center of Advanced Science and Technology, Beijing 100190, People's Republic of China*
[8]*COMSATS Institute of Information Technology, Lahore, Defence Road, Off Raiwind Road, 54000 Lahore, Pakistan*
[9]*G. I. Budker Institute of Nuclear Physics SB RAS (BINP), Novosibirsk 630090, Russia*
[10]*GSI Helmholtzcentre for Heavy Ion Research GmbH, D-64291 Darmstadt, Germany*
[11]*Guangxi Normal University, Guilin 541004, People's Republic of China*
[12]*Guangxi University, Nanning 530004, People's Republic of China*
[13]*Hangzhou Normal University, Hangzhou 310036, People's Republic of China*
[14]*Helmholtz Institute Mainz, Johann-Joachim-Becher-Weg 45, D-55099 Mainz, Germany*
[15]*Henan Normal University, Xinxiang 453007, People's Republic of China*
[16]*Henan University of Science and Technology, Luoyang 471003, People's Republic of China*
[17]*Huangshan College, Huangshan 245000, People's Republic of China*
[18]*Hunan University, Changsha 410082, People's Republic of China*
[19]*Indiana University, Bloomington, Indiana 47405, USA*
[20a]*INFN Laboratori Nazionali di Frascati, I-00044 Frascati, Italy*
[20b]*INFN and University of Perugia, I-06100 Perugia, Italy*
[21a]*INFN Sezione di Ferrara, I-44122 Ferrara, Italy*
[21b]*University of Ferrara, I-44122 Ferrara, Italy*
[22]*Institute of Physics and Technology, Peace Ave. 54B, Ulaanbaatar 13330, Mongolia*
[23]*Johannes Gutenberg University of Mainz, Johann-Joachim-Becher-Weg 45, D-55099 Mainz, Germany*
[24]*Joint Institute for Nuclear Research, 141980 Dubna, Moscow region, Russia*
[25]*Justus-Liebig-Universitaet Giessen, II. Physikalisches Institut, Heinrich-Buff-Ring 16, D-35392 Giessen, Germany*
[26]*KVI-CART, University of Groningen, NL-9747 AA Groningen, The Netherlands*
[27]*Lanzhou University, Lanzhou 730000, People's Republic of China*
[28]*Liaoning University, Shenyang 110036, People's Republic of China*
[29]*Nanjing Normal University, Nanjing 210023, People's Republic of China*
[30]*Nanjing University, Nanjing 210093, People's Republic of China*
[31]*Nankai University, Tianjin 300071, People's Republic of China*
[32]*Peking University, Beijing 100871, People's Republic of China*
[33]*Seoul National University, Seoul 151-747, Korea*
[34]*Shandong University, Jinan 250100, People's Republic of China*
[35]*Shanghai Jiao Tong University, Shanghai 200240, People's Republic of China*
[36]*Shanxi University, Taiyuan 030006, People's Republic of China*
[37]*Sichuan University, Chengdu 610064, People's Republic of China*
[38]*Soochow University, Suzhou 215006, People's Republic of China*
[39]*State Key Laboratory of Particle Detection and Electronics, Beijing 100049, Hefei 230026, People's Republic of China*
[40]*Sun Yat-Sen University, Guangzhou 510275, People's Republic of China*
[41]*Tsinghua University, Beijing 100084, People's Republic of China*
[42a]*Ankara University, 06100 Tandogan, Ankara, Turkey*
[42b]*Istanbul Bilgi University, 34060 Eyup, Istanbul, Turkey*
[42c]*Uludag University, 16059 Bursa, Turkey*
[42d]*Near East University, Nicosia, North Cyprus, Mersin 10, Turkey*
[43]*University of Chinese Academy of Sciences, Beijing 100049, People's Republic of China*
[44]*University of Hawaii, Honolulu, Hawaii 96822, USA*
[45]*University of Minnesota, Minneapolis, Minnesota 55455, USA*

[46]University of Science and Technology Liaoning, Anshan 114051, People's Republic of China
[47]University of Science and Technology of China, Hefei 230026, People's Republic of China
[48]University of South China, Hengyang 421001, People's Republic of China
[49]University of the Punjab, Lahore 54590, Pakistan
[50a]University of Turin, I-10125 Turin, Italy
[50b]University of Eastern Piedmont, I-15121 Alessandria, Italy
[50c]INFN, I-10125 Turin, Italy
[51]Uppsala University, Box 516, SE-75120 Uppsala, Sweden
[52]Wuhan University, Wuhan 430072, People's Republic of China
[53]Zhejiang University, Hangzhou 310027, People's Republic of China
[54]Zhengzhou University, Zhengzhou 450001, People's Republic of China

(Received 4 February 2018; published 10 April 2018)

We investigate the process $e^+e^- \to K\bar{K}J/\psi$ at center-of-mass energies from 4.189 to 4.600 GeV using 4.7 fb^{-1} of data collected by the BESIII detector at the BEPCII collider. The Born cross sections for the reactions $e^+e^- \to K^+K^-J/\psi$ and $K^0_SK^0_SJ/\psi$ are measured as a function of center-of-mass energy. The energy dependence of the cross section for $e^+e^- \to K^+K^-J/\psi$ is shown to differ from that for $\pi^+\pi^-J/\psi$ in the region around the $Y(4260)$. In addition, there is evidence for a structure around 4.5 GeV in the $e^+e^- \to K^+K^-J/\psi$ cross section that is not present in $\pi^+\pi^-J/\psi$.

DOI: 10.1103/PhysRevD.97.071101

The $Y(4260)$ resonance was first discovered in the process $e^+e^- \to Y(4260) \to \pi^+\pi^-J/\psi$ by the *BABAR* experiment [1] using the initial state radiation (ISR) technique and then later confirmed by CLEO [2] and Belle [3]. This state does not fit into the conventional charmonium spectrum of the quark model [4], which predicts three vector charmonium states in this mass region, usually identified as the experimentally established $\psi(4040)$, $\psi(4160)$, and $\psi(4420)$ states [5]. In addition, even though the mass of the $Y(4260)$ is well above the open-charm $D\bar{D}$ threshold, it has not yet been found to decay to $D\bar{D}$ [6], in contrast to the conventional charmonium states in this mass region. There are several theoretical interpretations of the $Y(4260)$, including tetraquark [7], meson molecule [8], hadroquarkonium [9], hybrid meson [10], and others [11].

In addition to $e^+e^- \to \pi^+\pi^-J/\psi$, the $Y(4260)$ state has been searched for in many other modes, including $\pi\pi h_c$ [12,13], $\omega\chi_{cJ}$ [14], $\eta J/\psi$ [15,16], $\eta' J/\psi$ [17] and $K\bar{K}J/\psi$ [18]. Rather than showing conclusive evidence for new $Y(4260)$ decay modes, the energy dependencies of the e^+e^- cross sections hint at a more complex pattern than just the existence of a $Y(4260)$. More recent results from BESIII, in the $\pi^+\pi^-J/\psi$ [19] and $\pi^+\pi^-h_c$ [20] final states, show two resonant structures within this region. In order to understand this mass region, it is thus important to measure additional e^+e^- cross sections. In particular, measuring the ratio of $K\bar{K}J/\psi$ and $\pi\pi J/\psi$ cross sections would allow us to gain new insight into the nature of the $Y(4260)$ [21].

In the following, we use 4.7 fb^{-1} of data collected at the Beijing spectrometer (BESIII) with center-of-mass energies ($E_{\rm CM}$) ranging from 4.189 to 4.600 GeV to measure the Born cross sections (σ) of the reactions $e^+e^- \to K^+K^-J/\psi$ and $K^0_SK^0_SJ/\psi$. To identify whether or not the K^+K^-J/ψ system originates from a $Y(4260)$, the energy dependence of the $e^+e^- \to K^+K^-J/\psi$ cross section is compared to that of $\pi^+\pi^-J/\psi$. The ratio $\sigma(K^0_SK^0_SJ/\psi)/\sigma(K^+K^-J/\psi)$ is also calculated to test isospin symmetry.

The BESIII experiment uses a general purpose magnetic spectrometer [22]. A superconducting solenoid magnet provides a 1.0 T field, enclosing a helium-gas-based drift chamber (MDC) for charged particle tracking, a plastic scintillator time-of-flight system (TOF) for particle identification (PID), and a CsI(Tl) electromagnetic calorimeter (EMC) to measure the energy of neutral particles. The

[a]Also at Bogazici University, 34342 Istanbul, Turkey.
[b]Also at the Moscow Institute of Physics and Technology, Moscow 141700, Russia.
[c]Also at the Functional Electronics Laboratory, Tomsk State University, Tomsk 634050, Russia.
[d]Also at the Novosibirsk State University, Novosibirsk 630090, Russia.
[e]Also at the NRC "Kurchatov Institute", PNPI, Gatchina 188300, Russia.
[f]Also at Istanbul Arel University, 34295 Istanbul, Turkey.
[g]Also at Goethe University Frankfurt, 60323 Frankfurt am Main, Germany.
[h]Also at Key Laboratory for Particle Physics, Astrophysics and Cosmology, Ministry of Education; Shanghai Key Laboratory for Particle Physics and Cosmology; Institute of Nuclear and Particle Physics, Shanghai 200240, People's Republic of China.
[i]Government College Women University, Sialkot—51310. Punjab, Pakistan.
[j]Currently at: Center for Underground Physics, Institute for Basic Science, Daejeon 34126, Korea.

Beijing Electron Positron Collider (BEPCII) uses two rings to collide electrons and positrons with $E_{\rm CM}$ from 2.0 to 4.6 GeV.

The data samples used in this analysis were collected at 14 different $E_{\rm CM}$ [23]. Large data sets were collected at 4.226 (1092 pb^{-1}), 4.258 (826 pb^{-1}), 4.358 (540 pb^{-1}), 4.416 (1074 pb^{-1}), 4.467 (110 pb^{-1}), 4.527 (110 pb^{-1}), and 4.600 (567 pb^{-1}) GeV. Other smaller samples of 50 pb^{-1} each were collected at 4.189, 4.208, 4.217, 4.242, 4.308, 4.387, and 4.575 GeV [24].

GEANT4-based [25] Monte Carlo (MC) simulations are used to study efficiencies and backgrounds. Signal MC samples are generated for $e^+e^- \to \pi^+\pi^- J/\psi$, $K^+K^- J/\psi$, and $K^0_S K^0_S J/\psi$ using EVTGEN [26] and assuming a phase space model for all decays. KKMC [27] is used to calculate the ISR correction factors needed to convert an observed cross section to a Born cross section [28,29].

Background MC samples are divided into three categories: quantum electrodynamic (QED), continuum, and peaking backgrounds. For the continuum backgrounds, samples are generated for $e^+e^- \to 4\pi$, 6π, $2K2\pi$, $2K4\pi$, and $p\bar{p}\pi\pi$. The cross sections for these channels were measured separately and were found to be on the order of 100 pb. For the peaking backgrounds, where a background J/ψ may be present, samples are generated for $e^+e^- \to \eta J/\psi, \eta' J/\psi, \pi^+\pi^-\psi(3686)$, and $\pi^0\pi^0\psi(3686)$ according to their known cross sections [15,17,30]. Other sources of backgrounds, including those from ISR or $D\bar{D}$, are also generated and are found to be negligible.

Final states in this analysis include $K^+K^- J/\psi$ and $K^0_S K^0_S J/\psi$, where the J/ψ decays into e^+e^- or $\mu^+\mu^-$, and each K^0_S decays into $\pi^+\pi^-$. In addition, the previously studied final state of $\pi^+\pi^- J/\psi$ [19,31] is reconstructed to cancel systematic uncertainties when calculating ratios of cross sections.

To select events, we require at least two positively charged and two negatively charged tracks for the $K^+K^- J/\psi$ and $\pi^+\pi^- J/\psi$ modes and at least three positively charged and three negatively charged tracks for the $K^0_S K^0_S J/\psi$ mode. If more than one combination passes the selection, multiple counting of events is allowed. However, our selection reduces combinatoric backgrounds to less than 0.5%, according to studies of the MC samples. A distance of closest approach for any primary charged track from the beam interaction point must be within ± 10 cm along the beam direction, and 1 cm in the plane perpendicular to the beam direction. The polar angle in the MDC for each charged track must satisfy $|\cos(\theta)| < 0.93$. To identify leptons, the energy deposited in the calorimeter divided by the momentum of any lepton candidate must be greater than 0.80 for either electron or less than 0.25 for both muons.

We perform a four-constraint (4C) kinematic fit for $\pi^+\pi^- J/\psi$ and $K^+K^- J/\psi$ and a six-constraint (6C) fit for $K^0_S K^0_S J/\psi$. For the 4C fits, the four-momentum is constrained to the initial center-of-mass system. For the 6C fits, the masses of the two K^0_S are also constrained. The resulting χ^2/dof is required to be less than 10.

To remove radiative Bhabha background events, where the radiated photon converts into an e^+e^- pair when interacting with the material inside the detector, all pairs of oppositely charged tracks must have an opening angle satisfying $\cos(\theta) < 0.98$. For PID, the TOF and ionization energy loss (dE/dx) from the MDC are combined to calculate probabilities for kaon and pion hypotheses of each track. The charged kaons in $K^+K^- J/\psi$ are selected by requiring ${\rm Prob}(K) > {\rm Prob}(\pi)$. This selection removes 90% of the continuum backgrounds while keeping 98% of the predicted signal. In the $K^0_S K^0_S J/\psi$ channel, in order to remove backgrounds from $e^+e^- \to \pi\pi\psi(3686)$ with $\psi(3686)$ decaying to $\pi^+\pi^- J/\psi$, each K^0_S must have $L/\sigma > 4$, where L is the K^0_S decay length and σ is its uncertainty. The π^+ and π^- pair from the K^0_S decay is required to have an invariant mass between 471 and 524 MeV/c^2 (roughly five times the mass resolution) and originate from a common vertex by requiring the χ^2 of a vertex fit be less than 100.

After the above selection, the distributions of dilepton invariant mass, ${\rm M}(l^+l^-)$, for the three different decay modes (with all 14 $E_{\rm CM}$ combined) are shown in Fig. 1. Clear J/ψ signals are observed. Backgrounds outside of the J/ψ signal region are well described by our background MC simulation and are flatly distributed. For $\pi^+\pi^- J/\psi$, the main background is from the process $e^+e^- \to \pi^+\pi^-\pi^+\pi^-$. For $K^+K^- J/\psi$, the main background is from $e^+e^- \to K^+K^-\pi^+\pi^-$. There are no significant peaking background events expected in any mode, with the largest estimated to be 0.4 events in the $K^0_S K^0_S J/\psi$ channel from $e^+e^- \to \pi^+\pi^-\psi(3686)$ $(\to \pi^+\pi^-\pi^+\pi^- J/\psi)$.

To explore potential intermediate states in the $K\bar{K}J/\psi$ channel, data are compared with phase-space signal MC events in Fig. 2. The signal MC histograms are normalized to the measured Born cross section at each $E_{\rm CM}$. There are no indications for peaking structures in the $K^\pm J/\psi$ mass distributions. In the K^+K^- invariant mass, however, there may be hints of $f_0(980)$ and $f_2(1270)$ signals, but there are not sufficient data to investigate further.

The Born cross section at each $E_{\rm CM}$ is calculated by

$$\sigma = \frac{N^{\rm sig}}{\mathcal{L}\epsilon(1+\delta)(1+\delta_{VP})B(J/\psi \to l^+l^-)}. \qquad (1)$$

The signal yield, $N^{\rm sig}$, is calculated by subtracting the number of J/ψ sideband events from the number of J/ψ signal events. The J/ψ signal region is $3084 < {\rm M}(l^+l^-) < 3116$ MeV/c^2; and the low and high sideband regions are $3004 < {\rm M}(l^+l^-) < 3068$ MeV/c^2 and $3132 < {\rm M}(l^+l^-) < 3196$ MeV/c^2, respectively. Uncertainties on the number of signal events are calculated using the Rolke method [32]. The total signal yields for all $E_{\rm CM}$ are 7984^{+99}_{-98} events for

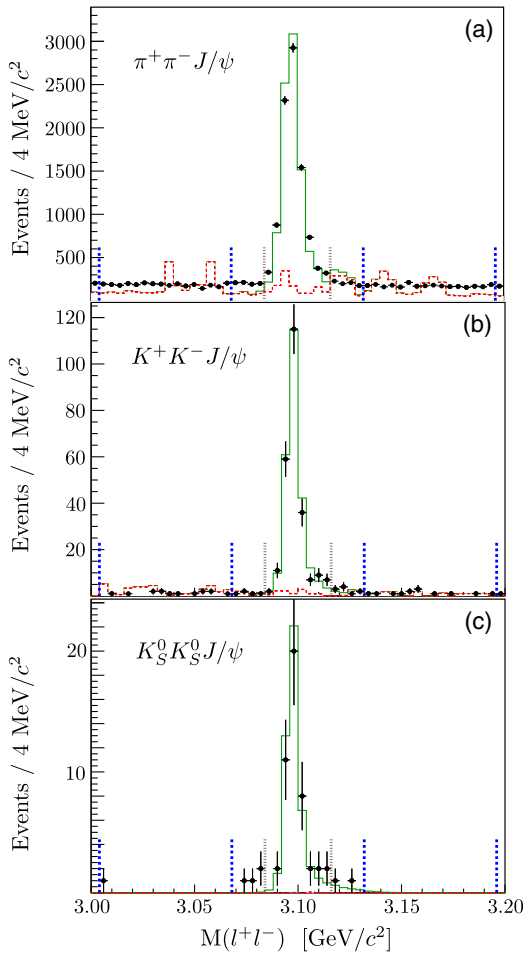

FIG. 1. The distribution of lepton pair mass, M(l^+l^-), for (a) $\pi^+\pi^- J/\psi$, (b) $K^+K^- J/\psi$, and (c) $K^0_S K^0_S J/\psi$. Data from all $E_{\rm CM}$ are combined. Points are for data; the green solid histograms are for signal MC events; and the red dashed histograms are for background MC events. The signal regions are shown by the gray dashed lines, while the sideband regions are shown with the blue dotted lines.

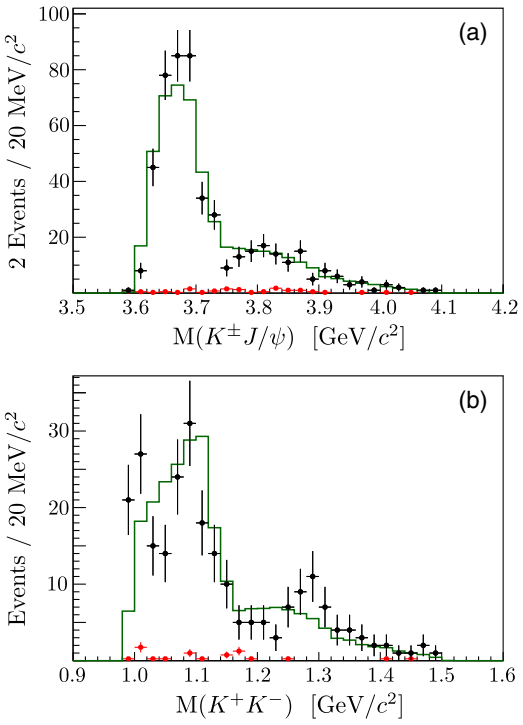

FIG. 2. The invariant mass distributions for (a) $K^\pm J/\psi$ (two entries per event) and (b) K^+K^-. Data from all $E_{\rm CM}$ are combined. Black points are for data from the J/ψ signal region; red points are for data from the J/ψ sideband regions (normalized to the size of the signal region); dark green solid histograms are for signal MC events (normalized using the measured cross section at each $E_{\rm CM}$).

the $\pi^+\pi^- J/\psi$ channel, 238^{+16}_{-15} for $K^+K^- J/\psi$, and $46.5^{+7.3}_{-6.6}$ for $K^0_S K^0_S J/\psi$. The integrated luminosity values, $\mathcal{L}$, are taken from Ref. [24]. The branching fraction $B(J/\psi \to l^+l^-) = (11.93 \pm 0.06)\%$ is taken from the particle data group (PDG) [5]. For the $K^0_S K^0_S J/\psi$ mode, a factor of $B(K^0_S \to \pi^+\pi^-)^2 = (47.9 \pm 0.03)\%$ is also included. The vacuum polarization factors, $(1 + \delta_{VP})$, are taken from Ref. [33]. The efficiencies for each mode, ϵ, are derived from the signal MC samples incorporating ISR effects. For $\pi^+\pi^- J/\psi$, the efficiencies (without ISR effects) at each energy point are around 48%. For $K^+K^- J/\psi$, the efficiencies range from 13% at low $E_{\rm CM}$ to 35% at high $E_{\rm CM}$. For $K^0_S K^0_S J/\psi$, the efficiencies are about 25%.

The ISR correction factors, $(1 + \delta)$, are calculated using an iterative procedure. A cross section following a Breit-Wigner line shape with PDG values for the mass and width of the $Y(4260)$ is used as the first input for both the $\pi^+\pi^- J/\psi$ and $K\bar{K}J/\psi$ channels. The resulting cross section line shapes are used as the next inputs, and this procedure is iterated until the Born cross section converges.

The results for $\sigma(\pi^+\pi^- J/\psi)$, $\sigma(K^+K^- J/\psi)$, and $\sigma(K^0_S K^0_S J/\psi)$ are shown in Figs. 3(a)–3(c) as functions of $E_{\rm CM}$ with both statistical and systematic uncertainties. To compare the shape of $\sigma(K^+K^- J/\psi)$ with $\sigma(\pi^+\pi^- J/\psi)$, we calculate the ratio $\sigma(K^+K^- J/\psi)/\sigma(\pi^+\pi^- J/\psi)$ [Fig. 3(d)]. If the $Y(4260)$ were the only contribution to the $\pi\pi J/\psi$ and $K\bar{K}J/\psi$ processes, this ratio would be slightly rising as a function of $E_{\rm CM}$ due to phase space factors. Instead, the observed ratio of cross sections falls with $E_{\rm CM}$. A constant ratio hypothesis is tested by fitting the ratio with a constant for samples with a high integrated luminosity, namely for $E_{\rm CM}$ of 4.226, 4.258, and 4.358 GeV. Based on the minimized χ^2 of 16.9 with two degrees of freedom and taking into account systematic errors on the ratio, we find a 3.5σ standard deviation discrepancy with the assumption of the observed ratio being a constant. We, therefore, cannot conclude that the $Y(4260)$ decays through $e^+e^- \to K\bar{K}J/\psi$.

In addition, Fig. 3(b) shows a peak near 4.5 GeV in $\sigma(K^+K^- J/\psi)$ that is not present in $\sigma(\pi^+\pi^- J/\psi)$. To test the discrepancy between the two channels, we fit $\sigma(K^+K^- J/\psi)/\sigma(\pi^+\pi^- J/\psi)$ at five $E_{\rm CM}$ from 4.416 to 4.600 GeV with a constant [Fig. 3(d)]. The resulting χ^2 of

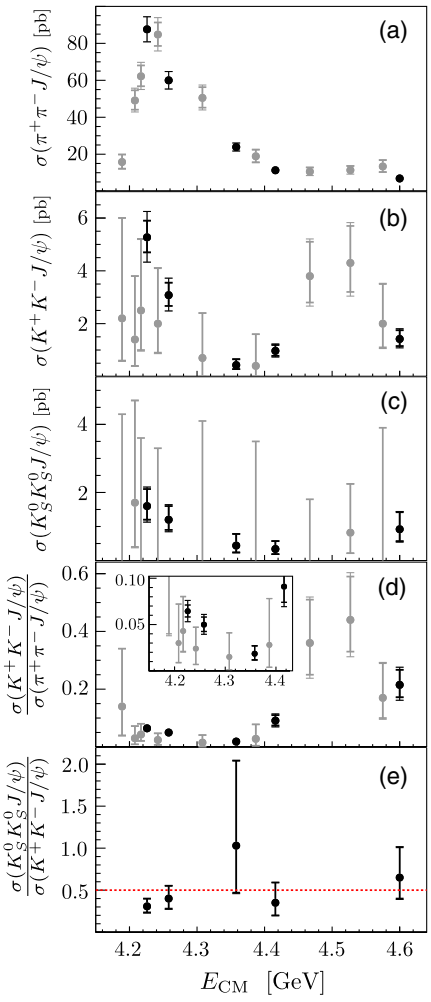

FIG. 3. The Born cross sections (a) $\sigma(\pi^+\pi^- J/\psi)$, (b) $\sigma(K^+K^- J/\psi)$, and (c) $\sigma(K^0_S K^0_S J/\psi)$, and the ratios (d) $\sigma(K^+K^- J/\psi)/\sigma(\pi^+\pi^- J/\psi)$, and (e) $\sigma(K^0_S K^0_S J/\psi)/\sigma(K^+K^- J/\psi)$. The black points are for data sets with high integrated luminosities; the gray points are for smaller data sets. Thicker error bars are for statistical uncertainties only; thinner error bars are for combined statistical and systematic uncertainties. In (c), the large error bars with no central point are 90% C.L. upper limits. In (d), the inset shows a narrower region of $E_{\rm CM}$. The red dotted line in (e) is the value expected from isospin symmetry.

the fit is 17.6 for four degrees of freedom, which indicates a 3.0σ standard deviation discrepancy from the assumption that the ratios are constant. There is thus evidence for a more complex structure in this region in $K^+K^- J/\psi$ than in $\pi^+\pi^- J/\psi$.

We also calculate the ratios between $\sigma(K^0_S K^0_S J/\psi)$ and $\sigma(K^+K^- J/\psi)$ for data samples with high luminosity. According to isospin symmetry, the ratio between these two modes should be $1/2$. The calculated ratios, along with this prediction, are shown in Fig. 3(e). The combined ratio over all energies, based on the total number of signal events, is $0.370^{+0.064}_{-0.058} \pm 0.042$, where the first uncertainty is statistical and the second is systematic. The five points shown in Fig. 3(e) are consistent with this average ratio with a χ^2 of 3.2 for four degrees of freedom.

Final results are listed in Table I. Upper limits are calculated at a 90% confidence level and incorporate systematic errors using the Rolke method with an additional uncertainty on the efficiency [32]. Systematic uncertainties in the Born cross section measurements are listed in Table II and are described below.

The integrated luminosity was measured with large-angle Bhabha events and the uncertainty is found to be less than 1% [24]. To account for the differences between data and MC simulation in the tracking and PID efficiency, a study was performed using the process $e^+e^- \to K^+K^-\pi^+\pi^-$. The systematic uncertainty is found to be 1.0% per charged pion and 2.5% per charged kaon. The relatively large uncertainty for the charged kaon efficiency is due to the momenta of the charged kaons in this analysis, which are smaller than in typical BESIII analyses. For the lepton tracking efficiency, a 1.0% uncertainty per lepton is applied [15]. We use J/ψ and K^0_S branching fractions from the PDG [5], which leads to systematic uncertainties of 0.5%. The K^0_S reconstruction efficiency is studied using control samples of $J/\psi \to K^0_S K^\pm \pi^\mp$ and $\phi K^0_S K^\pm \pi^\mp$. After factoring out uncertainties due to pion reconstruction and weighting according to the observed K^0_S momentum distributions, we find a 3.0% systematic uncertainty per K^0_S.

To study the efficiency of the kinematic fit requirements, we used control samples of $e^+e^- \to \pi^+\pi^-\pi^+\pi^-$, $K^+K^-\pi^+\pi^-$, and $K^0_S K^0_S \pi^+\pi^-$, which are similar to $\pi^+\pi^- J/\psi$, $K^+K^- J/\psi$, and $K^0_S K^0_S J/\psi$, respectively, but with higher statistics. Relative efficiencies are defined by comparing yields when requiring $\chi^2/{\rm dof} < 10$ versus $\chi^2/{\rm dof} < 100$. The differences in the efficiencies between MC simulation and data are 2.6% for $\pi^+\pi^-\pi^+\pi^-$, 3.8% for $K^+K^-\pi^+\pi^-$, and 5.9% for $K^0_S K^0_S \pi^+\pi^-$, which are taken as the systematic uncertainties.

To account for differences in J/ψ mass resolution between data and MC simulation, we smear the width of the J/ψ peak in the signal MC samples by 30%. The changes in the efficiencies of each mode are less than 1.0%, which are incorporated as a systematic uncertainty.

The uncertainty associated with the ISR correction factor is studied by replacing the iterative process, described previously, with a $Y(4260)$ Breit-Wigner cross section. The differences in the Born cross section between these two scenarios are 4.0% for $\pi\pi J/\psi$ and 6.0% for $K\bar{K} J/\psi$, which are taken as the uncertainty for the ISR correction. Uncertainties on the vacuum polarization corrections are estimated to be 0.5% according to Ref. [33].

To account for substructure in the $\pi\pi J/\psi$ mode, we compare the efficiency obtained with a phase-space MC sample to that for the process $e^+e^- \to \pi^\pm Z_c(3900)^\mp \to \pi^+\pi^- J/\psi$, using the PDG parameters for the $Z_c(3900)$. A 4.0% difference in efficiency is assigned as a conservative systematic uncertainty.

TABLE I. The center-of-mass energies ($E_{\rm CM}$), integrated luminosities ($\mathcal{L}$), and final results for $\sigma(K^+K^-J/\psi)$, $\sigma(K^0_SK^0_SJ/\psi)$, $\sigma(K^0_SK^0_SJ/\psi)/\sigma(K^+K^-J/\psi)$, and $\sigma(K^+K^-J/\psi)/\sigma(\pi^+\pi^-J/\psi)$. The first uncertainty is statistical, and the second is systematic. In the cases where there are zero signal events and zero sideband events, upper limits are calculated with 90% confidence levels and incorporate systematic uncertainties. The $\sigma(K^0_SK^0_SJ/\psi)/\sigma(K^+K^-J/\psi)$ ratio is only calculated for data samples with high integrated luminosity.

$E_{\rm CM}$ [GeV]	$\mathcal{L}$ [pb^{-1}]	$\sigma(K^+K^-J/\psi)$ [pb]	$\sigma(K^0_SK^0_SJ/\psi)$ [pb]	$\frac{\sigma(K^0_SK^0_SJ/\psi)}{\sigma(K^+K^-J/\psi)}$	$\frac{\sigma(K^+K^-J/\psi)}{\sigma(\pi^+\pi^-J/\psi)}$
4.189	43	$2.2^{+3.8}_{-1.6} \pm 0.3$	< 4.3	⋯	$0.14^{+0.20}_{-0.10} \pm 0.02$
4.208	55	$1.4^{+2.4}_{-1.0} \pm 0.2$	$1.7^{+3.0}_{-1.3} \pm 0.3$	⋯	$0.030^{+0.042}_{-0.021} \pm 0.004$
4.217	54	$2.5^{+2.7}_{-1.5} \pm 0.4$	< 3.6	⋯	$0.043^{+0.037}_{-0.022} \pm 0.006$
4.226	1092	$5.27^{+0.63}_{-0.57} \pm 0.75$	$1.6^{+0.5}_{-0.4} \pm 0.3$	$0.307^{+0.090}_{-0.072} \pm 0.034$	$0.064\,4^{+0.006\,7}_{-0.006\,2} \pm 0.0094$
4.242	56	$2.0^{+2.1}_{-1.1} \pm 0.3$	< 3.3	⋯	$0.024^{+0.023}_{-0.017} \pm 0.004$
4.258	826	$3.08^{+0.47}_{-0.41} \pm 0.44$	$1.2^{+0.4}_{-0.3} \pm 0.2$	$0.40^{+0.15}_{-0.12} \pm 0.05$	$0.049\,9^{+0.008\,2}_{-0.007\,4} \pm 0.0073$
4.308	45	$0.7^{+1.7}_{-0.7} \pm 0.1$	< 4.1	⋯	$0.015^{+0.026}_{-0.014} \pm 0.002$
4.358	540	$0.43^{+0.22}_{-0.15} \pm 0.06$	$0.44^{+0.34}_{-0.20} \pm 0.07$	$1.0^{+1.0}_{-0.6} \pm 0.1$	$0.018\,5^{+0.008\,3}_{-0.006\,5} \pm 0.0027$
4.387	55	$0.4^{+1.2}_{-0.4} \pm 0.1$	< 3.5	⋯	$0.028^{+0.050}_{-0.024} \pm 0.004$
4.416	1074	$0.97^{+0.22}_{-0.19} \pm 0.14$	$0.34^{+0.23}_{-0.15} \pm 0.05$	$0.35^{+0.24}_{-0.15} \pm 0.04$	$0.091^{+0.019}_{-0.017} \pm 0.013$
4.467	110	$3.8^{+1.3}_{-1.0} \pm 0.5$	< 1.8	⋯	$0.36^{+0.15}_{-0.11} \pm 0.05$
4.527	110	$4.3^{+1.4}_{-1.1} \pm 0.6$	$0.82^{+1.43}_{-0.60} \pm 0.13$	⋯	$0.44^{+0.15}_{-0.11} \pm 0.06$
4.575	48	$2.0^{+1.5}_{-0.9} \pm 0.3$	< 3.9	⋯	$0.17^{+0.12}_{-0.07} \pm 0.02$
4.600	567	$1.42^{+0.33}_{-0.27} \pm 0.20$	$0.92^{+0.50}_{-0.35} \pm 0.14$	$0.65^{+0.36}_{-0.25} \pm 0.07$	$0.215^{+0.052}_{-0.043} \pm 0.031$

For the $K\bar{K}J/\psi$ modes, there is an apparent discrepancy in the $K\bar{K}$ mass spectra between data and MC samples simulated with the phase-space model. We therefore weight the efficiency according to the observed $M(K^+K^-)$ distribution. This results in a 10% difference with respect to the nominal efficiency, which is assigned as a systematic uncertainty.

All of these uncertainties are summarized in Table II. The total systematic uncertainties are 7.6% for $\pi^+\pi^-J/\psi$, 14.2% for K^+K^-J/ψ, and 15.7% for $K^0_SK^0_SJ/\psi$. Taking into account correlations among uncertainties, the systematic uncertainty on the $\sigma(K^0_SK^0_SJ/\psi)/\sigma(K^+K^-J/\psi)$ ratio is 11.2% (the tracking and PID, K^0_S reconstruction, and kinematic fit uncertainties are uncorrelated) and that on the $\sigma(K^+K^-J/\psi)/\sigma(\pi^+\pi^-J/\psi)$ ratio is 14.8% (here the tracking and PID, kinematic fit, ISR, and substructure uncertainties are uncorrelated).

TABLE II. Summary of systematic uncertainties.

	$\pi^+\pi^-J/\psi$	K^+K^-J/ψ	$K^0_SK^0_SJ/\psi$
Luminosity	1.0%	1.0%	1.0%
Tracking and PID	4.0%	7.0%	6.0%
Branching ratios	0.5%	0.5%	0.5%
K^0_S reconstruction	⋯	⋯	6.0%
J/ψ resolution	1.0%	1.0%	1.0%
Kinematic fit	2.6%	3.8%	5.9%
Vacuum polarization	0.5%	0.5%	0.5%
ISR correction	4.0%	6.0%	6.0%
Z_c substructure	4.0%	⋯	⋯
KK substructure	⋯	10.0%	10.0%
Total	7.6%	14.2%	15.7%

In summary, we measure the Born cross sections as functions of $E_{\rm CM}$ for the processes $e^+e^- \to K^+K^-J/\psi$, $K^0_SK^0_SJ/\psi$, and $\pi^+\pi^-J/\psi$. We also measure the ratios of Born cross sections for $K^0_SK^0_SJ/\psi$ to K^+K^-J/ψ and K^+K^-J/ψ to $\pi^+\pi^-J/\psi$. The results suggest the K^+K^-J/ψ and $\pi^+\pi^-J/\psi$ cross sections have different energy dependencies in the region around the $Y(4260)$. In addition, there is evidence for an enhancement in the cross section of $e^+e^- \to K^+K^-J/\psi$ in the higher $E_{\rm CM}$ region. This is consistent with previous data [18]. Still, more data and additional analyses are needed to investigate the nature of this structure. We find the ratio of cross sections for the reactions with neutral and charged kaons to be consistent with expectations from isospin conservation.

ACKNOWLEDGMENTS

The BESIII Collaboration thanks the staff of BEPCII and the IHEP computing center for their strong support. This work is supported in part by National Key Basic Research Program of China under Contract No. 2015CB856700; National Natural Science Foundation of China (NSFC) under Contracts No. 11235011, No. 11322544,

No. 11335008, No. 11425524, and No. 11635010; the Chinese Academy of Sciences (CAS) Large-Scale Scientific Facility Program; the CAS Center for Excellence in Particle Physics (CCEPP); the Collaborative Innovation Center for Particles and Interactions (CICPI); Joint Large-Scale Scientific Facility Funds of the NSFC and CAS under Contracts No. U1232201, No. U1332201, No. U1532257, and No. U1532258; CAS under Contracts No. KJCX2-YW-N29, No. KJCX2-YW-N45; CAS Key Research Program of Frontier Sciences under Contract No. QYZDJ-SSW-SLH003; 100 Talents Program of CAS; National 1000 Talents Program of China; INPAC and Shanghai Key Laboratory for Particle Physics and Cosmology; German Research Foundation DFG under Contracts No. Collaborative Research Center CRC 1044, FOR 2359; Istituto Nazionale di Fisica Nucleare, Italy; Koninklijke Nederlandse Akademie van Wetenschappen (KNAW) under Contract No. 530-4CDP03; Ministry of Development of Turkey under Contract No. DPT2006K-120470; National Science and Technology Fund; The Swedish Research Council; U.S. Department of Energy under Contracts No. DE-FG02-05ER41374, No. DE-SC-0010118, No. DE-SC-0010504, No. DE-SC-0012069; University of Groningen (RuG) and the Helmholtzzentrum fuer Schwerionenforschung GmbH (GSI), Darmstadt; WCU Program of National Research Foundation of Korea under Contract No. R32-2008-000-10155-0.

[1] B. Aubert *et al.* (*BABAR* Collaboration), Phys. Rev. Lett. **95**, 142001 (2005).
[2] T. E. Coan *et al.* (CLEO Collaboration), Phys. Rev. Lett. **96**, 162003 (2006).
[3] C. Z. Yuan *et al.* (Belle Collaboration), Phys. Rev. Lett. **99**, 182004 (2007).
[4] T. Barnes, S. Godfrey, and E. S. Swanson, Phys. Rev. D **72**, 054026 (2005).
[5] C. Patrignani *et al.* (Particle Data Group Collaboration), Chin. Phys. C **40**, 100001 (2016).
[6] B. Aubert *et al.* (*BABAR* Collaboration), Phys. Rev. D **76**, 111105 (2007); G. Pakhlova *et al.* (Belle Collaboration), Phys. Rev. D **77**, 011103 (2008).
[7] L. Maiani, V. Riquer, F. Piccinini, and A. D. Polosa, Phys. Rev. D **72**, 031502 (2005).
[8] G. J. Ding, Phys. Rev. D **79**, 014001 (2009); Q. Wang, C. Hanhart, and Q. Zhao, Phys. Rev. Lett. **111**, 132003 (2013).
[9] S. Dubynskiy and M. B. Voloshin, Phys. Lett. B **666**, 344 (2008); X. Li and M. B. Voloshin, Mod. Phys. Lett. A **29**, 1450060 (2014).
[10] S. L. Zhu, Phys. Lett. B **625**, 212 (2005); F. E. Close and P. R. Page, Phys. Lett. B **628**, 215 (2005); E. Kou and O. Pene, Phys. Lett. B **631**, 164 (2005); L. Liu, G. Moir, M. Peardon, S. M. Ryan, C. E. Thomas, P. Vilaseca, J. J. Dudek, R. G. Edwards, B. Joó, and D. G. Richards(Hadron Spectrum Collaboration), J. High Energy Phys. 07 (2012) 126.
[11] F. K. Guo, C. Hidalgo-Duque, J. Nieves, and M. P. Valderrama, Phys. Rev. D **88**, 054007 (2013); L. Maiani, V. Riquer, R. Faccini, F. Piccinini, A. Pilloni, and A. D. Polosa, Phys. Rev. D **87**, 111102 (2013); E. Braaten, Phys. Rev. Lett. **111**, 162003 (2013); X. H. Liu and G. Li, Phys. Rev. D **88**, 014013 (2013).
[12] M. Ablikim *et al.* (BESIII Collaboration), Phys. Rev. Lett. **111**, 242001 (2013).
[13] M. Ablikim *et al.* (BESIII Collaboration), Phys. Rev. Lett. **113**, 212002 (2014).
[14] M. Ablikim *et al.* (BESIII Collaboration), Phys. Rev. Lett. **114**, 092003 (2015).
[15] M. Ablikim *et al.* (BESIII Collaboration), Phys. Rev. D **91**, 112005 (2015).
[16] X. L. Wang *et al.* (Belle Collaboration), Phys. Rev. D **87**, 051101 (2013).
[17] M. Ablikim *et al.* (BESIII Collaboration), Phys. Rev. D **94**, 032009 (2016).
[18] C. P. Shen *et al.* (Belle Collaboration), Phys. Rev. D **89**, 072015 (2014).
[19] M. Ablikim *et al.* (BESIII Collaboration), Phys. Rev. Lett. **118**, 092001 (2017).
[20] M. Ablikim *et al.* (BESIII Collaboration), Phys. Rev. Lett. **118**, 092002 (2017).
[21] C. F. Qiao, Phys. Lett. B **639**, 263 (2006).
[22] M. Ablikim *et al.* (BESIII Collaboration), Nucl. Instrum. Methods Phys. Res., Sect. A **614**, 345 (2010).
[23] M. Ablikim *et al.* (BESIII Collaboration), Chin. Phys. C **40**, 063001 (2016).
[24] M. Ablikim *et al.* (BESIII Collaboration), Chin. Phys. C **39**, 093001 (2015).
[25] S. Agostinelli *et al.* (GEANT4 Collaboration), Nucl. Instrum. Methods Phys. Res., Sect. A **506**, 250 (2003).
[26] D. J. Lange, Nucl. Instrum. Methods Phys. Res., Sect. A **462**, 152 (2001).
[27] S. Jadach, B. F. L. Ward, and Z. Was, Phys. Rev. D **63**, 113009 (2001).
[28] E. A. Kuraev and V. S. Fadin, Yad. Fiz. **41**, 733 (1985) [Sov. J. Nucl. Phys. **41**, 466 (1985)].
[29] R. G. Ping, Chin. Phys. C **38**, 083001 (2014).
[30] M. Ablikim *et al.* (BESIII Collaboration), Phys. Rev. D **96**, 032004 (2017); M. Ablikim *et al.* (BESIII Collaboration), arXiv:1710.10740.
[31] M. Ablikim *et al.* (BESIII Collaboration), Phys. Rev. Lett. **110**, 252001 (2013).
[32] W. A. Rolke, A. M. Lopez, and J. Conrad, Nucl. Instrum. Methods Phys. Res., Sect. A **551**, 493 (2005).
[33] S. Actis *et al.* (Working Group on Radiative Corrections and Monte Carlo Generators for Low Energies), Eur. Phys. J. C **66**, 585 (2010).